Skyrmions and Their Sizes in Helimagnets

Kwan-yuet Ho* and Theodore R. Kirkpatrick
Institute for Physical Science and Technology and Department of Physics, University of Maryland, College Park, MD 20742, USA

Dietrich Belitz
Department of Physics and Institute of Theoretical Science, University of Oregon, Eugene, Oregon 97403, USA

(Dated: December 30, 2011)

Skyrmion gases and lattices in helimagnets are studied, and the size of a Skyrmion in various phases is estimated. For isolated Skyrmions, the long distance tail is related to the magnetization correlation functions and exhibits power-law decay if the phase spontaneously breaks a continuous symmetry, but decays exponentially otherwise. The size of a Skyrmion is found to depend on a number of length scales. These length scales are related to the strength of Dzyaloshinskii-Moriya (DM) interaction, the thermal correlation lengths, and the strength of the external magnetic field. An Abrikosov lattice of Skyrmions is found to exist near the helimagnetic phase boundary, and the core-to-core distance is estimated.

PACS numbers: 12.39.Dc, 75.10.Hk, 75.50.-y

I. INTRODUCTION

Skyrmions are non-trivial topological objects in various field theories. They were first used to model baryons in nuclear physics.[1] More recently, they have been observed in quantum Hall ferromagnets,[2,3] p-wave superconductors,[4] and Bose-Einstein condensates.[5,6] The Skyrmion lattice is also a candidate for an experimentally observed periodic phase in helimagnets such as MnSi[7–9] (called the A phase) and $Fe_{1-x}Co_xSi$ (called the SkX phase).[10] The schematic phase diagram of a helimagnet is shown in Fig. 1. In these helimagnets, the usual ordered phase that exhibits long-range order takes the form of a helix,[11,12] that is thermodynamically stabilized by Dzyaloshinskii-Moriya (DM) interaction.[13,14] The helix of the magnet can be characterized by the pitch vector $\mathbf{q}$, with magnitude being the helical wavenumber and the direction being the direction of the helix. Its magnitude is proportional to the strength of the DM interaction. The phase that is believed to be a lattice of Skyrmions in these helimagnets have lattice size of the order of magnitude q^{-1}. It is likely that dilute Skyrmion gases in various phases of helimagnets can also be stabilized through the DM interaction.

An isolated Skyrmion is an exact solution of the saddle-point equation to the non-linear σ model.[16,17] Thermodynamically it is a metastable state. Different schemes have been proposed to stabilize the Skyrmions, with a dipole-dipole interaction[18] and a DM interaction[19–24] being two examples. These schemes introduce new physical length scales.

A lattice of Skyrmions has also been described as the superposition of three perpendicular helimagnets.[8,25] This Fourier description was argued to be a lattice of Skyrmion by calculating the Skyrmion density. However, this approximation is not a solution of the saddle-point equation to the model they are using.[15] Using the technique of Abrikosov vortices in type-II superconductors,[26] a lattice of Skyrmions can be described.[27] The Goldstone modes for such lattice is the same as that of the columnar phase of the liquid crystals.[28] Some previous studies[20,21] showed that by increasing the magnetic field, the system changes from aligned conical phase, then a Skyrmion lattice and finally to a ferromagnet. This is true for certain temperatures but not for all. The Skyrmion lattice is likely formed by a first-order phase transition.

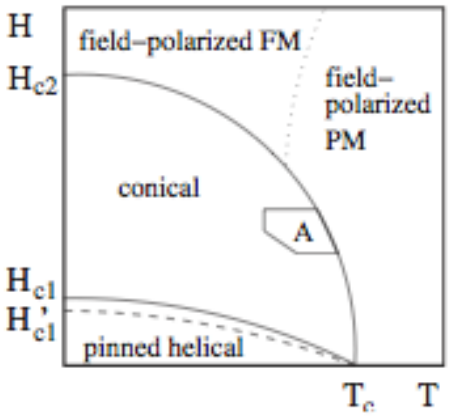

FIG. 1. Schematic phase diagram of MnSi in the H-T plane showing the helical, conical, and A phases, as well as the field-polarized ferromagnetic (FM) and paramagnetic (PM) states.[15]

The sizes of Skyrmions can be characterized in four ways. It can be characterized by the behavior near the core.[24] Alternatively, the size can also be characterized by the decay length of the long-distance tail of the Skyrmion. In this paper, we introduce yet another measure of the size of a of Skyrmion, which is given by the length at which the behaviors of the core and the tail

match. We believe that it is the best measure of the size of a Skyrmion. Finally, in a Skyrmion lattice, there is a fourth measure of the size of a Skyrmion: the distance between cores in the lattice.

In this paper, we study both an isolated Skyrmion and a Skyrmion lattice in the presence of DM interaction and external magnetic field, and we estimate their sizes. In Sec. II, we review the Landau-Ginzburg-Wilson (LGW) model with the DM interaction used to study the helimagnets. Crucially, we also introduce the various length scales in the problem. In Sec. III, we review the basic properties of Skyrmions, including the winding number. In Sec. IV, we study the core of isolated Skyrmions in various phases of the model. We find that for paramagnets and ferromagnets, the core behavior is readily found. The core behavior defines a measure of the core size, called R, which we find to be the result of the competition of different physical length scales in different regions of the phase diagram. We show that for the aligned conical phase, the core behavior is undetermined because of the scale invariance due to the spontaneous symmetry breaking. In Sec. V, we study the Skyrmion tails in various parts of the phase diagram. For paramagnets and ferromagnets, we find that the tail is exponentially decaying. The decay length of the tail depends on various length scales in different regions of the phase diagram. The Skyrmions in aligned conical phase, however, are algebraically decaying for large distances due to the underlying Goldstone modes in the system. In Sec. VI, we employ the Abrikosov flux lattice to study the Skyrmion lattice. We find that the core size depends on q and the thermal correlation length of paramagnets. In Sec. VII, we match the core and tail of Skyrmions, with the matching radius introduced as a new measure of the Skyrmion size. We argue that this measure of Skyrmion size is the most physical. In general, we find that the core size is of the order q^{-1} near the helimagnetic phase boundary, consistent with the results of other previous studies,[20,21] but it depends on other length scales in other parts of the phase diagram. We do not discuss pinning, polarization, and the alignment effects mentioned in a previous paper.[15]

II. MODEL AND LENGTH SCALES

A. LGW functional

Throughout this paper, we use the LGW model with DM Interaction[15]

$$\mathcal{S}[\mathbf{M}] = \int d^3x \left[\frac{r}{2}\mathbf{M}^2 + \frac{a}{2}(\nabla\mathbf{M})^2 + \frac{c}{2}\mathbf{M}\cdot\nabla\times\mathbf{M} + \frac{u}{4}(\mathbf{M}^2)^2 - \mathbf{H}\cdot\mathbf{M}\right]. \quad (1)$$

The terms with coefficients r, a and u are the usual Landau-Ginzburg-Wilson (LGW) model.[29] The c-term is the DM interaction[13,14], and it exists in systems with spin-orbit coupling[30] and no inversion symmetry in the unit cell of the solid.[12] A similar chiral structure can be found in cholestoric liquid crystal.[31] H is the external magnetic field. Its direction defines the z-axis throughout the paper. The saddle-point equation corresponding to Eq. (1) is[32]

$$r\mathbf{M} - a\nabla^2\mathbf{M} + c\nabla\times\mathbf{M} + uM^2\mathbf{M} - \mathbf{H} = 0, \quad (2)$$

We do not consider crystal-field effects in this paper. Generally these terms align the helix in a certain direction for small magnetic field. For large magnetic fields, the helix is in the direction of the field.

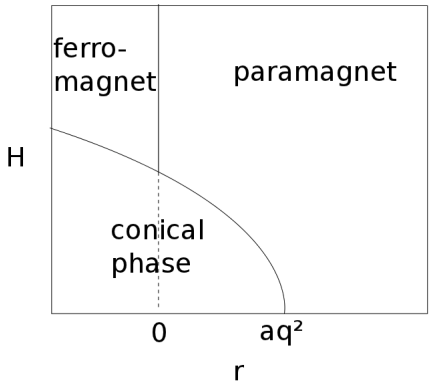

FIG. 2. Phase diagram predicted by the action in Eq. (1).

B. Phases and Length Scales

There are three topologically trivial phases that are associated with the action in Eq. (1). These three phases are the paramagnet, the ferromagnet and the aligned conical phase, as shown in Fig. (2). The aligned conical phase is stable only if $H \leq H_{c2}$ where H_{c2} is defined below, see Eq. (18).

1. *Paramagnet*

The paramagnet is stable or metastable only for $r > 0$. Its analytic form is given by Eq. (B2). In a magnetic field, the magnetization is

$$m = \chi_p H, \quad (3)$$

where $\chi_p = r^{-1}$ is the magnetic susceptibility. The corresponding correlation length is given by ξ_p, which diverges when r approaches 0. In LGW model, it is[29]

$$\xi_p = \sqrt{\frac{a}{r}}, \quad (4)$$

We define a length (basically the thermal and magnetic field dependent transverse correlation length)

$$\bar{l}_H = \sqrt{\frac{am}{H}}. \quad (5)$$

For $r \gg \frac{am}{H}$, it is

$$\bar{l}_H \approx \xi_p. \tag{6}$$

But for $r \ll \frac{am}{H}$, $m \approx (u^{-1}H)^{\frac{1}{3}}$. Hence the length becomes

$$\bar{l}_H \approx \frac{a^{\frac{1}{2}}}{u^{\frac{1}{6}}H^{\frac{1}{3}}}, \tag{7}$$

which is related to the mean-field critical exponent $\delta = 3$.[29]

2. Ferromagnet

The ferromagnet is stable or metastable only for $r < 0$. Its analytic form is given by Eq. (B4). Without external magnetic field, the magnetization is given by

$$M_F^{(0)} = \sqrt{\frac{|r|}{u}}. \tag{8}$$

A magnetic field along the direction of the magnet gives

$$m \approx M_F^{(0)} + \chi_f H, \tag{9}$$

where $\chi_f = (2|r|)^{-1}$ is the longitudinal susceptibility. The translational susceptibility goes like H^{-1}.

The longitudinal correlation length of the ferromagnet is given by

$$\xi_f = \sqrt{\frac{a}{2|r|}}, \tag{10}$$

which diverges for $r \to 0$. The transverse correlation length is given by $\bar{l}_H$ in Eq. (5). It is infinite for zero magnetic field, but in a field it is

$$\bar{l}_H \approx \frac{|r|^{\frac{1}{4}}a^{\frac{1}{2}}}{u^{\frac{1}{4}}H^{\frac{1}{2}}}. \tag{11}$$

3. Aligned Conical Phase

The aligned conical phase, or simply conical phase, contains a component of helicity and another of homogeneous magnetization, given by[15]

$$\mathbf{M}_{CP} = m_{sp}(\cos qz\hat{\mathbf{x}} + \sin qz\hat{\mathbf{y}}) + m_{//}\hat{\mathbf{z}}, \tag{12}$$

where q is the pitch vector of the helix given by

$$q = \frac{c}{2a}. \tag{13}$$

It is proportional to the strength of DM interaction. $m_{//}$ is the homogeneous magnetization induced by the magnetic field, and is given by

$$m_{//} = \chi_h H, \tag{14}$$

where $\chi_h = (aq^2)^{-1}$ is the magnetic susceptibility of the homogeneous magnetization. m_{sp} is the helimagnetic amplitude given by

$$m_{sp} = \sqrt{m_H^2 - m_{//}^2}, \tag{15}$$

where

$$m_H = \sqrt{\frac{aq^2 - r}{u}}. \tag{16}$$

The aligned conical phase can be the thermodynamically stable phase as in Fig. (2), if the system is in the region

$$aq^2 - r \geq \frac{uH^2}{a^2q^4}. \tag{17}$$

This defines the critical field H_{c2}

$$H_{c2} = aq^2\sqrt{\frac{aq^2 - r}{u}}. \tag{18}$$

At zero field, the correlation length approaching the helimagnetic-paramagnetic phase transition from the paramagnetic phase ($r > aq^2$) is given by

$$\xi_h = \sqrt{\frac{a}{r - aq^2}} = \left(\frac{1}{\xi_p^2} - q^2\right)^{-\frac{1}{2}}. \tag{19}$$

If the phase transition is approaching from the helimagnetic phase ($r < aq^2$), it is given by

$$\xi_h' = \sqrt{\frac{a}{aq^2 - r}} = \left(q^2 - \frac{1}{\xi_p^2}\right)^{-\frac{1}{2}}. \tag{20}$$

At the transition point between the helimagnet and paramagnet at $H = 0$,

$$q\xi_p = 1.$$

III. BASIC PROPERTIES OF SKYRMIONS

A. Winding Number

Skyrmions are two-dimensional objects, which are topologically non-trivial because the winding number of a Skyrmionic configuration is non-zero. Assume that

$$\mathbf{M}(\mathbf{x}) = m(\mathbf{x})\mathbf{n}(\mathbf{x}), \tag{21}$$

where $m(\mathbf{x})$ and $\mathbf{n}(\mathbf{x})$ denotes the magnitude and direction of $\mathbf{M}$. The winding number is defined as[33]

$$W = \int dx \int dy \frac{1}{4\pi}\mathbf{n} \cdot \left(\frac{\partial \mathbf{n}}{\partial x} \times \frac{\partial \mathbf{n}}{\partial y}\right). \tag{22}$$

Upon continuous deformation of the configurations, the winding number W remains unchanged. Note that all phases in Sec. II B have $W = 0$, which means they are all topologically trivial.

B. Description of Skyrmions

To illustrate a topologically non-trivial solution, we write the configuration in the form of[34] (in cylindrical coordinates)

$$\mathbf{n}(\mathbf{x}) = \sin\theta(\mathbf{x})\cos\alpha(\mathbf{x})\hat{\rho} + \sin\theta(\mathbf{x})\sin\alpha(\mathbf{x})\hat{\varphi} + \cos\theta(\mathbf{x})\hat{\mathbf{z}}, \tag{23}$$

so that the winding number can be written as

$$W = \frac{1}{4\pi}\int_0^\infty d\rho \int_0^{2\pi} d\varphi \cdot \sin\theta(\mathbf{x}) \left[-\frac{\partial\theta(\mathbf{x})}{\partial\varphi}\frac{\partial\alpha(\mathbf{x})}{\partial\rho} + \left(1 + \frac{\partial\alpha(\mathbf{x})}{\partial\varphi}\right)\frac{\partial\theta(\mathbf{x})}{\partial\rho}\right]. \tag{24}$$

For all the Skyrmions we review and present in this paper, $\theta(\rho = 0) = \pi$ and $\theta(\rho = \infty) = 0$, so that $W = -1$. In addition, we set $\alpha = \frac{\pi}{2}$, meaning it is an azimuthal Skyrmion. We exclude the consideration of a radial Skyrmion because the presence of DM interaction forces the Skyrmions be azimuthal. The winding number describes how the electron changes its spin when it passes through the core.[35] Such a Skyrmion is depicted in Fig. 3.

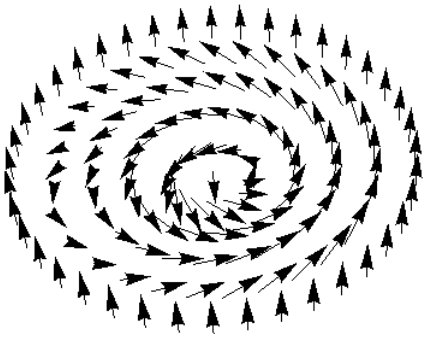

FIG. 3. The picture of an isolated azimuthal Skyrmion with $W = -1$.

Although Skyrmions are topological objects, linear response ensures that the asymptotic behaviors of the tails of Skyrmions are no different from the decay of other kinds of perturbations. It is the characteristics of the core that constitutes the topology. In understanding Skyrmions in various ordered phases of the helimagnets, we study the core by differential equations with boundary conditions that give a non-zero winding number, and the tail through perturbation theory.

IV. SKYRMION CORES

A. Ferromagnet and Paramagnet

We first explore the cases of paramagnets and ferromagnets. And as we have stated in Section III, $\theta(\rho = 0) = \pi$. Then we write, for $\rho \to 0$,

$$m(\mathbf{x}) = m_\infty + \delta m(\rho), \tag{25}$$

$$\theta(\mathbf{x}) = \pi + \delta\theta(\rho), \tag{26}$$

where all behavior depends only on the radial distance ρ, and where $m_\infty = M_P$ (for paramagnet, $r > 0$, as in Eq. (B2)) or M_F (for ferromagnet, $r < 0$, as in Eq. (B4)). Putting Eq. (25) and Eq. (26) in the saddle-point equations (D1) and (D2), ignoring all higher order terms, we can find that for $\rho \to 0$, $\delta\theta = \Theta_c\rho$ and $\delta m = M_c\rho^2$, with

$$M_c = \frac{m_\infty}{2\bar{l}_H^2(1 + 4q^2\bar{l}_H^2)}, \tag{27}$$

$$\Theta_c = -\frac{2q}{1 + 4q^2\bar{l}_H^2}, \tag{28}$$

where $\bar{l}_H$ is the transverse correlation length for paramagnets or ferromagnets in Eq. (6), Eq. (7) or Eq. (11). Note that this calculation breaks down if there is no DM interaction, or the Skyrmion is in an ordered phase.

The size of the core can be estimated with this solution as R, where $\theta = \pi\left(1 - \frac{\rho}{R}\right)$. Let us consider different cases in ferromagnets and paramagnets, and the relation of Skyrmion in paramagnets in some situations to the Skyrmion lattice.

1. *Ferromagnet*

For a ferromagnet with non-zero magnetic field, the core size R is given by the following cases (with the phase stable or metastable):

1. $\bar{l}_H \ll q^{-1}$: $R \approx \frac{\pi}{2q}$.

2. $q^{-1} \ll \bar{l}_H$: $R \approx 2\pi q\bar{l}_H^2$.

The first case refers to the region where the magnetic field is much larger than the critical field H_{c2}. The core size is proportional to q^{-1}. The second case refers to the region closer to $H = H_{c2}$, where the magnetic length $\bar{l}_H$ plays a role.

2. Paramagnet

For a paramagnet, the core size R is given by (in which the phase can be stable or metastable):

1. $\xi_p \ll q^{-1}$: $R \approx \frac{\pi}{2q}$.
2. $\xi_p \approx q^{-1}$ and along $H \approx H_{c2}$: $R \approx \frac{5\pi}{2q}$.

The magnetic field does not play a role in the core behavior for paramagnets. It is because close to $r \approx 0$, the paramagnet appears for $H > H_{c2}$ and $\bar{l}_H$ is less significant than the contribution of q^{-1}. For $r > \frac{am}{H}$, $\bar{l}_H \approx \xi_p$.

B. Aligned Conical Phase

The core behavior for aligned conical phase is different from paramagnets and ferromagnets in Sec. IV A because of the Goldstone mode in this phase. To understand it, we first study ferromagnet without external magnetic field and DM interaction. This is for illustrative purpose, because it breaks a continuous symmetry just like the conical phase does.

1. Ferromagnet without external magnetic field and DM interaction

With $H = 0$ and $q = 0$, the ferromagnet (with $r < 0$) is an ordered phase that breaks the continuous rotational symmetry of the action in Eq. (1). The differential equation for $\delta\theta$ in Eq. (26) as in Eq. (D2) becomes

$$\frac{d^2\delta\theta}{d\rho^2} + \frac{1}{\rho}\frac{d\delta\theta}{d\rho} - \frac{1}{\rho^2}\delta\theta = 0. \tag{29}$$

The differential equation is due to the gradient term in the action. Then

$$\delta\theta = A\rho, \tag{30}$$

with an arbitrary coefficients A. In fact, the approximation in Eq. (C7) from the exact Skyrmion solution to the non-linear σ model near the core gives the same. Therefore, we cannot determine the core size. To determine the core size just from the core behavior, external perturbations that provide extra length scales are needed. For example, the presence of DM interaction fixes l in Eq. (C7) to be $(4q)^{-1}$.

2. Aligned Conical Phase

The aligned conical phase breaks the continuous translational symmetry of the action in Eq. (1).[15] Because of the helical nature of this phase, we expect $m(\mathbf{x})$, $\theta(\mathbf{x})$ and $\alpha(\mathbf{x})$ depend on ξ (defined in Eq. (D3)) in addition to the radial distance ρ. After analyzing Eqs. (D4), (D5) and (D6), the dominant variation near the core is $\rho\sin\xi$. However, the coefficients is undetermined for the same reason as Sec. IV B 1. The perturbation for conical phase can be written as Eq. (41). The differential equations for the fluctuations for conical phase can be written as a Laplace equation as in Eq. (42), although both gradient terms and curl term (due to DM interaction) in the action in Eq. (1) are important for the aligned conical phase.

V. SKYRMION TAILS

The tail behavior of the Skyrmions is closely related to the correlations in the bulk of the phase.[36] This can be shown by linear response theory (see Appendix E). In the following, we show by each case that the presence of spontaneous symmetry breaking gives the Skyrmion an algebraic tail, but an exponentially decaying tail otherwise. The decay length of the tail is in general not the same as the core size.

A. Paramagnet and Ferromagnet

We study the system using perturbation techniques. As we have stated in Section III, $\theta(\rho = \infty) = 0$. Then we write, for $\rho \to \infty$,

$$m(\mathbf{x}) = m_\infty + \delta m(\rho), \tag{31}$$
$$\theta(\mathbf{x}) = 0 + \delta\theta(\rho), \tag{32}$$

where all behavior depends only on the radial distance ρ, and $m_\infty = M_P$ (for paramagnet, $r > 0$, as in Eq. (B2)) or M_F (for ferromagnet, $r < 0$, as in Eq. (B4)) as in Sec. IV. We expect that the tail is exponential. Hence, we assume $\delta m = \tilde{M}e^{-K\rho}$ and $\delta\theta = \Theta e^{-K\rho}$. One of the solutions for K, called K_-, is used to define the length of the tail

$$l_T = \frac{1}{|K_-|}, \tag{33}$$

which is another measure of the size of Skyrmions. In some cases, K_- has an imaginary part, which indicates the tails are oscillating in addition to the exponential decay, but we will omit oscillations below despite its existence in some cases.

1. Ferromagnet

For ferromagnet, the lengths of the Skyrmion tails are:

1. $\bar{l}_H \ll q^{-1} \ll \xi_f$: $l_T \approx \bar{l}_H$.
2. $\bar{l}_H \ll \xi_f \ll q^{-1}$ and $\xi_f \ll \bar{l}_H \ll q^{-1}$: $l_T \approx \bar{l}_H$.

For both cases, the tails has a length $l_T \sim H^{-\frac{1}{2}}$ as in Eq. (11). We expect this because the transverse fluctuations of ferromagnet have the spectrum $\omega(\mathbf{k}) = k^2 + H$.[15]

2. Paramagnet

For paramagnet, the lengths of the tails are:

1. $\bar{l}_H \ll q^{-1} \ll \xi_p$: $l_T \approx \bar{l}_H$.
2. $\xi_p \ll q^{-1} \ll \bar{l}_H$: $l_T \approx \xi_p$.
3. $\xi_p \lesssim q^{-1}$ and small H: $l_T \approx \xi_h$.
4. Along $H \approx H_{c2}$: $l_T \approx \frac{\sqrt{2}}{\kappa_-}$,

where for the fourth case,

$$\kappa_\pm = \sqrt{q\sqrt{q^2+\frac{2}{\xi_h'^2}} \pm \left(q^2 - \frac{1}{\xi_h'^2}\right)}. \tag{34}$$

The first case corresponds to the the paramagnet with large magnetic field and the boundary with ferromagnet, where $\bar{l}_H$ is given by Eq. (6). The second case refers to the paramagnet far away from the transition points, making $l_T \approx \xi_p$. The third case refers to the paramagnet very close to the helimagnetic transition point, making $l_T \approx \xi_h$.

The fourth case refers to the paramagnet along $H \approx H_{c2}$. The Skyrmion lattice is formed along part of this critical line.

B. Aligned Conical Phase

By Goldstone theorem and linear response, any perturbation in the conical phase shows long distance algebraic decay. Therefore, a Skyrmion in this phase shows a long tail. For illustrative purpose, we study the ferromagnet without magnetic field and DM interaction which breaks the rotational symmetry.

1. Ferromagnet without external magnetic field and DM interaction

The spectrum of the Goldstone modes in ferromagnet in $H = 0$ and $q = 0$ is $\omega(\mathbf{k}) = k^2$,[29] and the modes are readily diagonalized as δm_x and δm_y. As a result, they behaves $|\mathbf{r}|^{-1}$, as illustrated in Appendix E. We expect the Skyrmion tail to behave in the same way.

We still employ the perturbation schemes in Eq. (31) and Eq. (32) for this ferromagnet with $H = 0$ and $q = 0$. The differential equations kept to the relevant order is given as

$$\frac{\partial^2\delta m}{\partial\rho^2} + \frac{1}{\rho}\frac{\partial\delta m}{\partial\rho} - M_F^{(0)}\left(\frac{\partial\delta\theta}{\partial\rho}\right)^2 - \frac{M_F^{(0)}}{\rho^2}(\delta\theta)^2 = \frac{\delta m}{\xi_f^2}, \tag{35}$$

$$\frac{\partial^2\delta\theta}{\partial\rho} + \frac{1}{\rho}\frac{\partial\delta\theta}{\partial\rho} - \frac{1}{\rho^2}\delta\theta = 0. \tag{36}$$

From an analysis of the differential equations (D1) and (D1), we get

$$\delta\theta = \frac{\Theta_f}{\rho}, \tag{37}$$

$$\delta m = -2\xi_f^2 M_F^{(0)}\frac{\Theta_f^2}{\rho^4}. \tag{38}$$

From Eq. (36), we know that the coefficients Θ_f is arbitary, as in core solution the coefficients in Eq. (30) in Sec. IV B 1 is undetermined as well. It is the result of the equation for the fluctuations given by a Laplace equation for a symmetry-breaking ferromagnet. $\delta m(\rho)$ and $\delta\theta(\rho)$ can be expressed in the scaling form $f\left(\frac{\xi_f^2}{L^2}, \frac{\rho}{L}\right)$, for some length scale L. Moreover, the approximation in Eq. (C7) far from the Skyrmion core in the non-linear σ model has the same behavior. Similarly, as in the Skyrmion core, the coefficients can be fixed by additional interactions that carry other length scales as discussed in Sec. IV B 1.

2. Aligned Conical Phase

While the ferromagnet has the readily diagonalized Goldstone modes with spectrum $\omega(\mathbf{k}) = k^2$, the aligned conical phase has the Goldstone modes given by[15]

$$\omega(\mathbf{k}) \approx k_z^2 + \frac{\xi_h'^{-2}}{q^2+\xi_h'^{-2}}\left(\frac{H}{H_{c2}}\right)^2\mathbf{k}_\perp^2 + \left[1 - \frac{4}{q^2\xi_h'^2}\left(\frac{H}{H_{c2}}\right)^2\right]\frac{\mathbf{k}_\perp^4}{2q^2}, \tag{39}$$

for small magnetic field ($m_{//}^2 \ll m_H^2$), similar to that of the cholesteric liquid crystal.[31] For zero magnetic field makes, the second term vanishes.[37] For the parametrization of fluctuations about the conical phase (12) can be written as[15]

$$\begin{aligned}\mathbf{M}(\mathbf{x}) = m_{sp}\,&[\cos(qz+\varphi_0(\mathbf{x}))\hat{\mathbf{x}} + \sin(qz+\varphi_0(\mathbf{x}))\hat{\mathbf{y}} \\ &+(\varphi_+(\mathbf{x})\cos qz + \varphi_-(\mathbf{x})\sin qz)\hat{\mathbf{z}}] \\ &+m_{//}[\pi_1(\mathbf{x})\hat{\mathbf{x}} + \pi_2(\mathbf{x})\hat{\mathbf{y}} + \hat{\mathbf{z}}],\end{aligned} \tag{40}$$

to the first order of all parameters. The Goldstone mode that corresponds to (39) is given by the "diagonalized" form as

$$\begin{aligned}&\delta m_G(\mathbf{x}) \\ &\approx \phi_0(\mathbf{x}) - \frac{q^2+\xi_h'^{-2}\left[1-\left(\frac{H}{H_{c2}}\right)^2\right]}{q(q^2+\xi_h'^{-2})}\frac{\partial\varphi_+(\mathbf{x})}{\partial y} \\ &+\frac{q^2+\xi_h'^{-2}\left[1-\left(\frac{H}{H_{c2}}\right)^2\right]}{q(q^2+\xi_h'^{-2})}\frac{\partial\varphi_-(\mathbf{x})}{\partial x} \\ &-\frac{\xi_h'^{-2}\left[1-\left(\frac{H}{H_{c2}}\right)^2\right]}{q(q^2+\xi_h'^{-2})}\frac{\partial\pi_1(\mathbf{x})}{\partial x} + \frac{\xi_h'^{-2}\left[1-\left(\frac{H}{H_{c2}}\right)^2\right]}{q(q^2+\xi_h'^{-2})}\frac{\partial\pi_2(\mathbf{x})}{\partial y},\end{aligned} \tag{41}$$

which satisfies the partial differential equation

$$\left[\frac{\partial^2}{\partial z^2}+\frac{\xi_h'^{-2}}{q^2+\xi_h'^{-2}}\left(\frac{H}{H_{c2}}\right)^2\nabla_\perp^2\right]\delta m_G(\mathbf{x})\approx 0, \quad (42)$$

for $H\neq 0$.[38] Eq. (42) has a solution

$$\delta m_G(\mathbf{x})=\frac{A}{\rho}\sin(\varphi+B), \quad (43)$$

with undetermined coefficients A and B. (Note that the Skyrmion core in conical phase has arbitrary size R and goes like $\rho\sin(\varphi+B)$ for the same argument.) Therefore, similar to ferromagnets, the Skyrmion tail in the conical phase has a power law form. A detailed analysis of the saddle-point equations in Appendix D 2 shows that Skyrmion tail in the conical phase goes like $\rho^{-1}\sin\xi$, where ξ is defined in Eq. (D3), with arbitrary coefficients.

VI. SKYRMION LATTICE

In this section, we study a lattice of Skyrmion in helimagnets. It is convenient to use CP^1 representation because Skyrmions are like vortices in superconductors and the technique of Abrikosov lattice of vortices can be used. The details of this representation can be found in Appendix A. The saddle-point equations in this representation are Eq. (A6) and Eq. (A7).

In Eq. (A7), the gauge $\mathbf{A}$ depends on $\mathbf{z}$ as in Eq. (A4), leading to the non-linearity. To fix the gauge, set $\mathbf{A}=-hx\hat{\mathbf{y}}$. The dimension of h is that of the reciprocal of area, and it will be shown later that it is related to the area of a Skyrmion core. Because of the periodic nature of the lattice, the term $-iqmn_\alpha\partial_\alpha z_i\to -iqm\langle n_\alpha\rangle\partial_\alpha z_i$ is ignored. This can be justified by the final solution. The term $-\frac{i}{2}qmz_i\partial_\alpha n_\alpha$ is also zero because the Skyrmions are azimuthal. Moreover, instead of keeping strictly $\mathbf{z}^\dagger\mathbf{z}=1$, we relax the condition to $\langle\mathbf{z}^\dagger\mathbf{z}\rangle=1$ where the average is over one lattice. Following Abrikosov,[26] one part of the solution is given by[27]

$$\mathbf{z}=\sqrt{\frac{\frac{h}{3^{\frac{1}{4}}\pi}}{1+|d_0|^2}}e^{iky}e^{-\frac{h}{2}\left(x+\frac{k}{h}\right)^2}\begin{bmatrix}1\\ d_0\sqrt{2h}\left(x+\frac{k}{h}\right)\end{bmatrix}, \quad (44)$$

where the prefactor is for normalization, and

$$d_0=-\frac{iq}{\sqrt{2h}}\frac{1}{\frac{1}{2}+\frac{H}{4ahm}+\sqrt{\frac{1}{4}+\frac{q^2}{2h}+\frac{H}{4ahm}+\left(\frac{H}{4ahm}\right)^2}}.$$

Let l_x and l_y be the distances between cores along the x and y axes respectively, where $l_xl_y=\frac{2\pi}{h}$. Then $\mathbf{z}$ can be seen as the superposition of the above solution with different values of k where $k_j=\frac{2\pi j}{l_y}$, then

$$\mathbf{z}=\sqrt{\frac{\frac{h}{3^{\frac{1}{4}}\pi}}{1+|d_0|^2}}\sum_{j=-\infty}^{\infty}c_je^{i\frac{2\pi j}{l_y}y}e^{-\frac{h}{2}(x+jl_x)^2}\begin{bmatrix}1\\ d_0\sqrt{2h}\,(x+jl_x)\end{bmatrix} \quad (45)$$

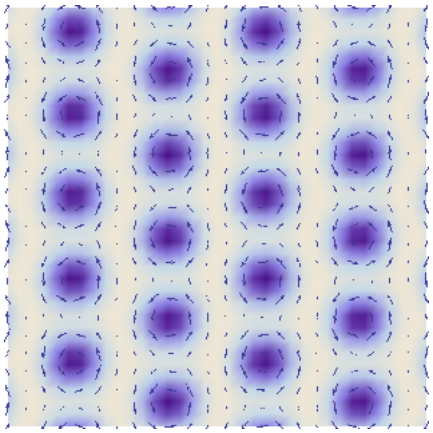

FIG. 4. Hexagonal Skyrmion lattice described by (45), for $h\sim q^2$, where the vectors denote the projection of the spin on the plane, and the color denotes $n_z=z_i^*\sigma_z^{ij}z_j$ where deep blue denotes spin reversed from the magnetic field.

For a triangular lattice, $c_j=c_{j+2}$[39]. Choose c_j to be $\frac{1}{\sqrt{2}}$ and $\frac{i}{\sqrt{2}}$ for even and odd j's. And $l_y=\frac{\sqrt{3}}{2}l_x$. Such configuration is plotted as shown in Fig. 4 for $h\sim q^2$, which denotes a Skyrmion lattice. On the other hand, a graph with spin projected on the basal plane (x-y plane) and a density plot of $n_z=z_i^*\sigma_z^{ij}z_j$ is plotted in Fig. 4.

To know the magnetization and the core size, we have to put Eq. (45) back to Eq. (A5) and determine them by variational method. Since the lattice is periodic, it is valid and convenient to consider the solution of a single site in Eq. (44). Define

$$\tilde{h}=\frac{h}{q^2},$$
$$\mathcal{D}=\left[\frac{1}{2}+\frac{H}{4aq^2m\tilde{h}}+\sqrt{\frac{1}{4}+\frac{1}{2\tilde{h}}+\frac{H}{4aq^2m\tilde{h}}+\left(\frac{H}{4aq^2m\tilde{h}}\right)^2}\right]^{-1},$$

the free energy per unit volume of one Skyrmion in the lattice is given by

$$\frac{\mathcal{F}}{V}=\frac{r}{2}m^2+\frac{u}{4}m^4+aq^2m^2\frac{\tilde{h}\left(1+\frac{3\mathcal{D}^2}{2\tilde{h}}\right)-2\mathcal{D}}{1+\frac{\mathcal{D}^2}{2\tilde{h}}}-Hm\frac{1-\frac{\mathcal{D}^2}{2\tilde{h}}}{1+\frac{\mathcal{D}^2}{2\tilde{h}}}. \quad (46)$$

Then we evaluate magnetization m and the reciprocal of core area h by minimizing the free energy. There exists no analytic closed form solution for m and h, but we do it by qualitative analysis. We expect that m is of the same order of magnitude of $m_{//}$ in the aligned conical phase or the paramagnet, and $\frac{h}{q^2}<1$. Expanding Eq. (46) for small $\frac{h}{q^2}$, we get

$$\frac{\mathcal{F}}{V}\approx\frac{r}{2}m^2+\frac{u}{4}m^4-Hm+aq^2m^2\left(\frac{h}{q^2}\right)-\frac{4a^3q^6m^4}{H^2}\left(\frac{h}{q^2}\right)^2.$$

Minimizing it with respect to h and m, we get

$$\frac{h}{q^2} \approx \frac{H^2}{8a^2q^4m^2},$$
$$rm + um^3 - H \approx 0.$$

The second equation indicates that the magnetization is approximately equal to the paramagnet or ferromagnet. For small magnetic field and in the paramagnetic phase ($r > 0$), using Eq. (B2), we get

$$h \approx \frac{1}{8q^2\xi_p^4}. \tag{47}$$

Therefore, the core-to-core distance goes like $q\xi_p^2$. Near the helimagnetic phase boundary $\xi_p q \approx 1$, and in this region the core-to-core distance goes like q^{-1}.

The experimentally observed A phase[7] that has been identified as hexagonal lattice of Skyrmions is observed along the helimagnet/paramagnet phase boundary,[8,10]. Our result shows that the core size $\sim q\xi_p^2$, which is $\sim q^{-1}$ for $q\xi_p \approx 1$, agreeing with previous theoretical[8,20,22,24,27] and experimental studies.[7,10] However, we also predict that the size increases away from the phase boundary, provided the Skyrmion lattice is still the thermodynamic ground state when the correlation length ξ_p gets larger.

The fluctuations due to the Skyrmion lattice has the same form of that of columnar phase in liquid crystal,[28] and have the form $\omega(\mathbf{k}) = \mathbf{k}_\perp^2 + c_1k_z^2 + c_2k_z^4$.[15]

VII. CORE SIZE AS THE MATCHING DISTANCE BETWEEN CORE BEHAVIOR AND SKYRMION TAIL

The definition of R in Sec. IV A deals only with the core behavior. Here we introduce a new distance L, which is defined as tbe distance where the core behavior and tail of the Skyrmion meet. By finding L, we consider both the core and the tail of the Skyrmion. In some cases, R and L are not too different in terms of order of magnitudes, but their difference becomes greater when the magnetic field becomes large.

In the following cases, we match the core behavior and the tail at a point L, and then we solve for L.

A. Paramagnet and Ferromagnet

For paramagnet and ferromagnet, by matching the core behavior in Sec. IV and the tail in Sec. V, we solve for the matching point L tabulated in Table I. We verify that for all cases in Table I have winding number $W = -1$, by putting the solutions of $\theta(\mathbf{x})$ back to Eq. (24).

From Table I, we can see that R's are mostly of the order of magnitude of q^{-1}, and l_T's are mostly the thermal correlation lengths. However, L shows much more complicated dependence on the various length scales. l_T is generally not a good measure of a Skyrmion size because the correlation length is related to the thermodynamic phase of the bulk, the size of an additional object. Both R and L is of the order of magnitude of q^{-1} near the helimagnetic transition point at $H \approx 0$, indicating that the Skyrmion size is of q^{-1} in this region. Far from this point, L and R differs in orders of magnitude. In general, L is better to characterize the size of Skyrmions because it takes into account both the core and the tail. Whether L or R is a better measure depends on the situations, as listed below:

1. If L and R are of the same order of magnitude ($\sim K^{-1}$ or oscillating) as in Fig. 5 (a), they are equally good. Examples: paramagnets in $q^{-1} \ll \bar{l}_H \ll \xi_p$ and $\xi_p \lesssim q^{-1}$.

2. If $R \gg L$ as in Fig. 5 (b), L is a better measure because L depicts where the tail starts and the slope of the core behavior was underestimated. Examples: ferromagnets in $\xi_f \ll q^{-1} \ll \bar{l}_H$, $\xi_f \ll \bar{l}_H \ll q^{-1}$, $\bar{l}_H \ll \xi_f \ll q^{-1}$ and $\bar{l}_H \ll q^{-1} \ll \xi_f$, and paramagnets in $\bar{l}_H \ll q^{-1} \ll \xi_p$ and $\xi_p \ll q^{-1} \ll \bar{l}_H$.

3. If $L \gg R$ as in Fig. 5 (c), R is a better measure. The matching method is not working so well because at $\rho = L$, $\theta(\rho)$ becomes negative. However, There are no such examples in all cases considered in Table I.

Therefore, for our purpose, L is a better characterization of the Skyrmion size in general.

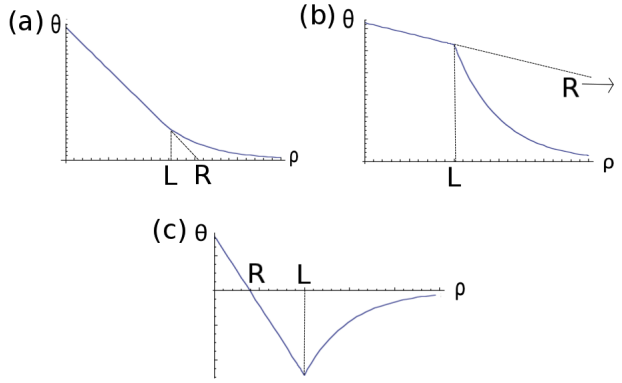

FIG. 5. Plots for $\theta(\rho)$ for Skyrmions in paramagnets and ferromagnets, and the meanings of R and L as the sizes of the Skyrmion core. (a) $R \approx L$. Both are equally good measures for the core size. (b) $R \gg L$. L is a better measure for the core size. (c) $R \ll L$. R is a better measure for the core size.

For pure ferromagnets ($q = 0$ and $H = 0$) and aligned conical phase, matching does not fix the size of the Skyrmion due to the same reason stated in Sec. V B 1. For pure ferromagnets, matching the solutions in Eq. (C7) for small and large ρ does not give L.

TABLE I. Isolated Skyrmions in ferromagnets and paramagnets in different regions of the phase diagram in Fig. 2. (PM = paramagnet, FM = ferromagnet)

PM/FM	Region in Phase Diagram	l_T	R	L
FM	$\xi_f \ll q^{-1} \ll \bar{l}_H$	$\bar{l}_H$	$2\pi q\bar{l}_H^2$	$\sqrt{32\pi q^3\bar{l}_H^3\xi_f}$
FM	$\xi_f \ll \bar{l}_H \ll q^{-1}$	$\bar{l}_H$	$\frac{\pi}{2q}$	$\sqrt{4\pi q\bar{l}_H\xi_f}$
FM	$\bar{l}_H \ll \xi_f \ll q^{-1}$	$\bar{l}_H$	$\frac{\pi}{2q}$	$\sqrt{2\pi q\bar{l}_H\bar{l}_H}$
FM	$\bar{l}_H \ll q^{-1} \ll \xi_f$	$\bar{l}_H$	$\frac{\pi}{2q}$	$\sqrt{2\pi q\bar{l}_H\bar{l}_H}$
PM	$\xi_p \ll q^{-1} \ll \bar{l}_H$	ξ_p	$\frac{\pi}{2q}$	$\frac{[2\pi(q\xi_p)^2]^{\frac{1}{3}}}{q}$
PM	$q^{-1} \ll \bar{l}_H \ll \xi_p$	$q^{-2}\bar{l}_H^{-1}$	$2\pi q\bar{l}_H^2$	$2\pi q\bar{l}_H^2$
PM	$\bar{l}_H \ll q^{-1} \ll \xi_p$	$\bar{l}_H$	$\frac{\pi}{2q}$	$\sqrt{2\pi q\bar{l}_H\bar{l}_H}$
PM	$\xi_p \lesssim q^{-1}$	ξ_h	$\frac{5\pi}{2q}$	$1.48q^{-1}$
PM	Along $H \approx H_{c2}$	$\frac{\sqrt{2}}{\kappa_-}$	$\frac{5\pi}{2q}$	$\frac{\pi}{\sqrt{2}\kappa_+}$

B. Aligned Conical Phase

Because of the technical complexities of aligned conical phase, we do not match the core and tail solutions as we did for other magnets. However, we assume a form of Syrmionic solution here and estimate the range of the core size. We describe an isolated Skyrmion in terms of

$$\begin{aligned}\mathbf{M} = [1-\eta_1(\rho,\xi)]m_{sp}(\cos qz\hat{\mathbf{x}} + \sin qz\hat{\mathbf{y}}) \\ +m_{//}\hat{\mathbf{n}}_{sk} - \eta_3(\rho,\xi)m_{//}\hat{\mathbf{z}},\end{aligned} \tag{48}$$

where $\hat{\mathbf{n}}_{sk}$ is the same Skyrmion in (Eqs. C1-C3). The first and third term are with variational parameters η_1 and η_3 which does not alter the winding number. The second term with $\hat{\mathbf{n}}_{sk}$ keeps the winding number to be -1. Because Eq. (48) already captures the long-range behavior as $\hat{\mathbf{n}}_{sk}\cdot(-\sin qz\hat{\mathbf{x}} + \cos qz\hat{\mathbf{y}}) \sim \frac{1}{\rho}\sin\xi$ far from the core ($\rho\to\infty$), there is no term in the direction of $(-\sin qz\hat{\mathbf{x}} + \cos qz\hat{\mathbf{y}})$ in Eq. (48).

We then solve for η_1 and η_3 by putting Eq. (48) to the saddle-point equation (2) for regions far from the core ($\rho\to\infty$) and near the core ($\rho\approx 0$). Far from the core ($\rho\to\infty$), we find that

$$\eta_1 \approx \frac{(3aq^2-2r)m_{//}}{2um_{sp}^3}\left(\frac{2l}{\rho}\sin\xi\right), \tag{49}$$

$$\eta_3 \approx -\frac{m_{//}}{m_{sp}}\left(\frac{2l}{\rho}\sin\xi\right), \tag{50}$$

where l is an undetermined parameter that we estimate below. At the core ($\rho\approx 0$), with linearization of the parameters in the saddle-point equation (2), we find that

$$\eta_1 \approx -E_1\left(\frac{2\rho}{l}\sin\xi\right), \tag{51}$$

$$\eta_3 \approx 1 - B_3\left(\frac{\rho}{l}\right)^2 - E_3\left(\frac{2\rho}{l}\sin\xi\right), \tag{52}$$

where (in terms of bare parameters in the action)

$$\begin{aligned}E_1 = &\frac{\left[r(1-lq)+\frac{4a}{l^2}(2-q^2l^2)\right]m_{//}}{r-\frac{2aq}{l}+u(3m_{sp}^2+4m_{//}^2)} \\ &-\frac{2u(m_{//}^2-2m_{sp}^2)m_{//}m_{sp}^2}{(7m_{//}^2-4m_{sp}^2)\left[r-\frac{2aq}{l}+u(3m_{sp}^2+4m_{//}^2)\right]} \\ &-\frac{uql(28m_{//}^5-23m_{//}^3m_{sp}^2+4m_{//}m_{sp}^4)}{(7m_{//}^2-4m_{sp}^2)\left[r-\frac{2aq}{l}+u(3m_{sp}^2+4m_{//}^2)\right]},\end{aligned} \tag{53}$$

$$\begin{aligned}B_3 = &\frac{4qlm_{sp}^2}{7m_{//}^2-4m_{sp}^2} \\ &+\frac{l^2\left(\frac{4a}{l^2}-\frac{4aq}{l}+r-4um_{//}^2+um_{sp}^2\right)}{2a},\end{aligned} \tag{54}$$

$$E_3 = \frac{4m_{//}m_{sp}}{7m_{//}^2-4m_{sp}^2}. \tag{55}$$

Then we match Eq. (49) and Eq. (51), and η_3 by matching Eq. (50) and Eq. (52) at some distance $\rho = L$, and we can solve for l. Matching is only possible if B_3 and E_3 are positive, and E_1 is negative. For E_3 to be positive, the denominator $7m_{//}^2 - 4m_{sp}^2$ has to be positive. (This makes the Skyrmion gas to appear only if $H \geq 0.798H_{c2}$.) L depends on ξ slightly. The lack of an analytic solution forces us to explore the core size numerically.

In Table II, the sizes of Skyrmions in the aligned conical phase with different values of the correlation length ξ_h' and $H = 0.8H_{c2}$ are listed. L is the size of a Skyrmion found by matching method. It depends on the phase angle ξ but it does not vary significantly. In general, as the system goes away from the phase boundary (as ξ_h' decreases), the size of the Skyrmion decreases.

TABLE II. Isolated Skyrmions in aligned conical phase for different values of ξ_h' all for $H = 0.8H_{c2}$.

ξ_h'	l	L	$\xi = qz - \varphi$
$3.16q^{-1}$ ($r = 0.7aq^2$)	$1.59q^{-1}$	$2.38q^{-1}$	0
	$1.59q^{-1}$	$2.31q^{-1}$	$\frac{\pi}{2}$
	$1.59q^{-1}$	$2.38q^{-1}$	π
	$1.58q^{-1}$	$2.24q^{-1}$	$\frac{3\pi}{2}$
$1.83q^{-1}$ ($r = 0.7aq^2$)	$1.13q^{-1}$	$2.13q^{-1}$	0
	$1.13q^{-1}$	$1.88q^{-1}$	$\frac{\pi}{2}$
	$1.13q^{-1}$	$2.13q^{-1}$	π
	$1.12q^{-1}$	$1.38q^{-1}$	$\frac{3\pi}{2}$
$1.41q^{-1}$ ($r = 0.5aq^2$)	$0.88q^{-1}$	$1.35q^{-1}$	0
	$0.88q^{-1}$	$1.29q^{-1}$	$\frac{\pi}{2}$
	$0.88q^{-1}$	$1.35q^{-1}$	π
	$0.88q^{-1}$	$1.23q^{-1}$	$\frac{3\pi}{2}$
$1.29q^{-1}$ ($r = 0.4aq^2$)	$0.79q^{-1}$	$1.13q^{-1}$	0
	$0.79q^{-1}$	$1.15q^{-1}$	$\frac{\pi}{2}$
	$0.79q^{-1}$	$1.13q^{-1}$	π
	$0.80q^{-1}$	$1.20q^{-1}$	$\frac{3\pi}{2}$

VIII. SUMMARY AND CONCLUSION

In summary, we have studied various aspects of Skyrmions in helimagnets. We first studied the Skyrmion core, and a related measure of core size R for paramagnets and ferromagnets. For the aligned conical phase, this R becomes arbitrary. Extra perturbations are needed to determine it. We then discussed the Skyrmion tails. They decay exponentially for paramagnets and ferromagnets. We determined their decay lengths l_T, which is another measure of the size of Skyrmion. We cannot define l_T for the aligned conical phase because the Skyrmions have algebraic tails, as expected from Goldstone theorem. We also studied the lattice of Skyrmions. Through variational methods, we found that the core-to-core distance in the lattice is of the order of magnitude $q\xi_p^2$. This can be compared with the experimentally observed A phase where the core-to-core distance is found to be $\sim q^{-1}$. Insofar as $q\xi_p \approx 1$ near the helimagnetic phase boundary, experimental and theoretical results agree. Lastly, we introduced the matching radius L, as another measure of the core size. In our studies, the core sizes are of the order q^{-1} near the helimagnetic phase boundary, consistent with various previous studies. However, in other parts of the phase diagram, it depends on other length scales as well such as the thermal correlation lengths ξ_p or ξ_f, and the magnetic length $\bar{l}_H$, as shown in Table I. Among all measures of sizes of Skyrmions, we think that L is the best because it depends on the whole Skyrmion. We also estimated the size of Skyrmions in aligned conical phase by matching. It is also of order q^{-1} near the helimagnetic phase boundary, and decreases away from it.

ACKNOWLEDGMENTS

This work was supported by the National Science Foundation under Grants No. DMR-09-29966 and No. DMR-09-01907.

Appendix A: Model in CP^1 Representation

To facilitate the study of topologically non-trivial Skyrmions, it is useful to write the model in terms of the CP^1 representation, which is commonly used in the study of quantum Hall ferromagnets.[2] We first write

$$\mathbf{M}(\mathbf{x}) = m(\mathbf{x})\mathbf{n}(\mathbf{x}), \tag{A1}$$

where $m(\mathbf{x})$ and $\mathbf{n}(\mathbf{x})$ denotes the magnitude and direction of $\mathbf{M}$. The direction $\mathbf{n}$ can be written in terms of two-component spin through the Hopf mapping:[40]

$$n_\alpha = z_i^* \sigma_\alpha^{ij} z_j, \tag{A2}$$

where σ_α is the Pauli matrix. From now onwards, Greek indices denote spatial component and Latin indices denote merely matrix component in spins. The constraint $\mathbf{n}^2 = 1$ gives

$$z_i^* z_i = 1. \tag{A3}$$

Because $\mathbf{n}$ has a definite magnitude, there are only two degrees of freedom. Therefore, $\mathbf{z}$ should have two degrees of freedom only, accomplished by the constraint Eq. (A3) and fixing the gauge[27]

$$A_\alpha = -\frac{i}{2}(z_i^* \partial_\alpha z_i - z_i \partial_\alpha z_i^*), \tag{A4}$$

such that the transformation $z_i(\mathbf{x}) \to e^{-i\theta(\mathbf{x})} z_i(\mathbf{x})$ and $z_i^*(\mathbf{x}) \to e^{i\theta(\mathbf{x})} z_i^*(\mathbf{x})$ does not lead to a change in the physical system.

In this representation, we write the action in Eq. (1) as

$$\begin{aligned}
&\mathcal{S}[m, \mathbf{A}, \mathbf{z}] \\
&= \int d^3x \left[\frac{r}{2}m^2 + \frac{u}{4}m^4 + \frac{a}{2}\partial_\alpha m \partial_\alpha m - H_\alpha m z_i^* \sigma_\alpha^{ij} z_j\right] \\
&\quad + 2am^2 \left[(\partial_\alpha z_i^*)(\partial_\alpha z_i) - A_\alpha A_\alpha\right] \\
&\quad + cm^2 \left[z_i^* \sigma_\alpha^{ij} z_j A_\alpha + \frac{i}{2}(\partial_\alpha z_i^*)\sigma_\alpha^{ij} z_j - \frac{i}{2} z_i^* \sigma_\alpha^{ij} \partial_\alpha z_j\right]
\end{aligned} \tag{A5}$$

The saddle-point equation associated with this representation has to be done with Lagrangian multiplier because of the constraint in Eq. (A3). Consider $\mathcal{S} + \lambda \int d^3x (z_i^* z_i - 1)$ with λ being the Lagrangian multiplier, the saddle-point equations are

$$(r-3aq^2-4aA_\alpha A_\alpha)m-a\partial_\alpha\partial_\alpha m-4aqmn_\alpha A_\alpha+um^3-H_\alpha n_\alpha+4am\left[\left(\delta_{ij}\partial_\alpha-\frac{iq}{2}\sigma^{ij}_\alpha\right)z^*_j\right]\left[\left(\delta_{ik}\partial_\alpha+\frac{iq}{2}\sigma^{ik}_\alpha\right)z_k\right]=0, \tag{A6}$$

$$m\left(\delta_{ij}\partial_\alpha-i\delta_{ij}A_\alpha+\frac{iq}{2}\sigma^{ij}_\alpha\right)\left(\delta_{jk}\partial_\alpha-i\delta_{jk}A_\alpha+\frac{iq}{2}\sigma^{jk}_\alpha\right)z_k-iqm\left(n_\alpha\partial_\alpha z_i+\frac{1}{2}z_i\partial_\alpha n_\alpha\right)+\frac{1}{2a}H_\alpha\sigma^{ij}_\alpha z_j=\lambda z_i. \tag{A7}$$

Appendix B: Analytic Expressions for the Paramagnet and the Ferromagnet in Mean-field LGW Model

For the paramagnet and the ferromagnet, the magnetization can be solved by the saddle-point equation derived from LGW functional,

$$rm+um^3-H=0. \tag{B1}$$

Its analytic solutions are given in the following.

1. Paramagnet

The paramagnet phase is only valid for $r>0$. Its full analytic expression is given by

$$M_P=\chi_p H f\left(\sqrt{\frac{u}{r^3}}H\right), \tag{B2}$$

where

$$f(x)=\frac{1}{x}\left[\frac{x}{2}+\sqrt{\frac{1}{27}+\left(\frac{x}{2}\right)^2}\right]^{\frac{1}{3}}+\frac{1}{x}\left[\frac{x}{2}-\sqrt{\frac{1}{27}+\left(\frac{x}{2}\right)^2}\right]^{\frac{1}{3}}. \tag{B3}$$

A Taylor's expansion for small H confirms that $M_p\approx\chi_p H$ as in Eq. (3). However, when r approaches 0, $M_p\approx\left(\frac{H}{u}\right)^{\frac{1}{3}}$, giving the critical exponent $\delta=3$ for the mean-field theory.[29]

2. Ferromagnet

The ferromagnet is only for $r<0$. In general the magnetization is given by

$$M_F=\begin{cases} M_F^{(0)}\left(\cos\frac{\gamma}{3}+\frac{1}{\sqrt{3}}\sin\frac{\gamma}{3}\right), & \text{for } H<\frac{2}{\sqrt{27}|r|}\sqrt{\frac{u}{|r|}} \\ 2\chi_f H f\left(\sqrt{\frac{u}{|r|^3}}H\right), & \text{for } H>\frac{2}{\sqrt{27}|r|}\sqrt{\frac{u}{|r|}} \end{cases} \tag{B4}$$

where $M_F^{(0)}$ is given by Eq. (8), $f(x)$ is defined in (B3) and

$$\sin\gamma=\frac{\sqrt{27}}{2|r|}\sqrt{\frac{u}{|r|}}H. \tag{B5}$$

A Taylor's expansion for small H confirms that $m\approx M_F^{(0)}+\chi_f H$.

Appendix C: Isolated Skyrmion in Non-Linear σ Model

In the ferromagnetic phase, the fluctuations can be studied with non-linear σ model.[41] In this model, there exists a metastable mean-field solution that corresponds to a Skyrmion given by[17]

$$n_x=-\frac{2l\rho\sin\varphi}{l^2+\rho^2}, \tag{C1}$$

$$n_y=\frac{2l\rho\cos\varphi}{l^2+\rho^2}, \tag{C2}$$

$$n_z=\frac{\rho^2-l^2}{\rho^2+l^2}. \tag{C3}$$

where l is an arbitrary length that characterizes the size of the Skyrmion core. In terms of the representation in Eq. (23),[4]

$$\alpha(\mathbf{x})=\frac{\pi}{2}, \tag{C4}$$

$$\theta(\mathbf{x})=2\tan^{-1}\frac{l}{\rho}. \tag{C5}$$

In CP^1 representation,

$$\mathbf{z}=\sqrt{\frac{\rho^2}{\rho^2+l^2}}\begin{bmatrix} e^{i\left(\frac{\pi}{2}-\varphi\right)} \\ \frac{l}{\rho}\end{bmatrix}, \tag{C6}$$

which is an anti-vortex.[27] This solution has a winding number $W=-1$,[16] confirming that it is a Skyrmion.

This Skyrmion in non-linear σ model states that

$$\theta(\rho)\approx\begin{cases}\pi-\frac{\rho}{2l}, & \text{for } \rho\approx 0 \\ \frac{2l}{\rho}, & \text{for } \rho\to\infty.\end{cases} \tag{C7}$$

We cannot determine l as discussed in Sec. IV B 1.

Appendix D: Saddle-Point Equations for $m(\mathbf{x})$, $\theta(\mathbf{x})$ and $\alpha(\mathbf{x})$

1. In Field-Polarized Magnets

Putting $\mathbf{M}=m\mathbf{n}$ with $\mathbf{n}$ given by Eq. (23) with $\alpha(\mathbf{x})=\frac{\pi}{2}$ into Eq. (2), the saddle-point equation becomes

$$rm-a\left[\left(\frac{\partial^2 m}{\partial\rho^2}+\frac{1}{\rho}\frac{\partial m}{\partial\rho}\right)-m\left(\frac{\partial\theta}{\partial\rho}\right)^2-\frac{1}{\rho^2}m\sin^2\theta\right]$$

$$+cm\left(\frac{\partial\theta}{\partial\rho}+\frac{1}{\rho}\sin\theta\cos\theta\right)+um^3-H\cos\theta=0, \tag{D1}$$

$$am\left(\frac{\partial^2\theta}{\partial\rho^2}+\frac{1}{\rho}\frac{\partial\theta}{\partial\rho}-\frac{1}{\rho^2}\sin\theta\cos\theta+\frac{2}{m}\frac{\partial m}{\partial\rho}\frac{\partial\theta}{\partial\rho}\right)+c\left(\frac{\partial m}{\partial\rho}+\frac{1}{\rho}m\sin^2\theta\right)-H\sin\theta=0. \tag{D2}$$

These two equations are useful for describing a Skyrmion in paramagnets and ferromagnets.

2. In helimagnetic phases

Putting $\mathbf{M}=m\mathbf{n}$ with $\mathbf{n}$ given by Eq. (23) and with

$$\xi=qz-\varphi, \tag{D3}$$

the Eq. (2) gives the following equations:

$$\begin{aligned}rm_s\sin\theta\cos\alpha-a\left\{\frac{1}{\rho}\frac{\partial}{\partial\rho}\left[\rho\frac{\partial}{\partial\rho}(m_s\sin\theta\cos\alpha)\right]\right\}\\-a\left\{\left(\frac{1}{\rho^2}+q^2\right)\frac{\partial^2}{\partial\xi^2}(m_s\sin\theta\cos\alpha)+\frac{2}{\rho^2}\frac{\partial}{\partial\xi}(m_s\sin\theta\sin\alpha)-\frac{1}{\rho^2}m_s\sin\theta\cos\alpha\right\}\\+c\left[-\frac{1}{\rho}\frac{\partial}{\partial\xi}(m_s\cos\theta)-q\frac{\partial}{\partial\xi}(m_s\sin\theta\sin\alpha)\right]+um_s^3\sin\theta\cos\alpha=0,\end{aligned} \tag{D4}$$

$$\begin{aligned}rm_s\sin\theta\sin\alpha-a\left\{\frac{1}{\rho}\frac{\partial}{\partial\rho}\left[\rho\frac{\partial}{\partial\rho}(m_s\sin\theta\sin\alpha)\right]\right\}\\-a\left\{\left(\frac{1}{\rho^2}+q^2\right)\frac{\partial^2}{\partial\xi^2}(m_s\sin\theta\sin\alpha)-\frac{2}{\rho^2}\frac{\partial}{\partial\xi}(m_s\sin\theta\cos\alpha)-\frac{1}{\rho^2}m_s\sin\theta\sin\alpha\right\}\\+c\left[-\frac{\partial}{\partial\rho}(m_s\cos\theta)+q\frac{\partial}{\partial\xi}(m_s\sin\theta\cos\alpha)\right]+um_s^3\sin\theta\sin\alpha=0,\end{aligned} \tag{D5}$$

$$\begin{aligned}rm_s\cos\theta-a\left\{\frac{1}{\rho}\frac{\partial}{\partial\rho}\left[\rho\frac{\partial}{\partial\rho}(m_s\cos\theta)\right]+\left(\frac{1}{\rho^2}+q^2\right)\frac{\partial^2}{\partial\xi^2}(m_s\cos\theta)\right\}\\+c\left[\frac{1}{\rho}\frac{\partial}{\partial\rho}(\rho m_s\sin\theta\sin\alpha)+\frac{1}{\rho}\frac{\partial}{\partial\xi}(m_s\sin\theta\cos\alpha)\right]+um_s^3\cos\theta-H=0.\end{aligned} \tag{D6}$$

Appendix E: Linear Response Theory

Linear response theory relates external perturbations of a physical system to the correlation functions in the unperturbed one.[36] This ensures that the perturbations have long-ranged behaviors if there exist correlation functions for massless modes for fluctuations. In contrast, the perturbations are of short-ranged if there do not exist any massless modes. This explains the behaviors of Skyrmion tails in different phases in Sec. V in relation to the Goldstone theorem.

Assume there is a field $\mathbf{M}(\mathbf{x})$ with a known mean-field solution $\mathbf{M}_0$, with the corresponding free energy per temperature being S_0. Let the kernel matrix for fluctuations be $\mathbf{K}(\mathbf{x},\mathbf{x}')$ and an external perturbation $\mathbf{H}(\mathbf{x})$. Then the corresponding partition function is

$$Z=e^{-S_0}\int D\mathbf{M}\cdot\exp\left[-\int d^dx\int d^dx'\frac{1}{2}\delta M_i(\mathbf{x})K_{ij}(\mathbf{x},\mathbf{x}')\delta M_j(\mathbf{x}')+\beta\int d^dx\cdot H_i(\mathbf{x})\delta M_i(\mathbf{x})\right], \tag{E1}$$

where summation is on repeated indices and $\beta=(k_BT)^{-1}$. By carrying out the functional integral, we get the fluctuation determinant.[42] The equation for δM, by variational principle, is

$$\int d^dx'\cdot K_{ij}(\mathbf{x},\mathbf{x}')\delta M_j(\mathbf{x}')-\beta H_i(\mathbf{x})=0, \tag{E2}$$

and hence,

$$\delta M_i(\mathbf{x})=\beta\int d^dx'\cdot K^{-1}_{ij}(\mathbf{x},\mathbf{x}')H_j(\mathbf{x}'). \tag{E3}$$

Note that the inverse of the kernel matrix is actually the correlation matrix. We can see from here that the perturbation $\delta\mathbf{M}(\mathbf{x})$ has the same behavior as the correlation

functions $\mathbf{K}(\mathbf{x},\mathbf{x}')$. If $K^{-1}(\mathbf{x},\mathbf{x}') = K^{-1}(\mathbf{x}-\mathbf{x}')$, the Fourier representation of Eq. (E3) is

$$\delta M_i(\mathbf{k}) = \beta K_{ij}^{-1}(\mathbf{k}) H_j(\mathbf{k}). \tag{E4}$$

We illustrate this with the example of a pure ferromagnet with $q = 0$ and $H = 0$. Assume that the magnet is aligned along z direction. Then the kernel matrices (the inverse of the correlation functions) are given by[29]

$$K_{ij}(\mathbf{k}) = \delta_{ij}(ak^2 - 2r\delta_{jz}).$$

This indicates that along x and y directions, the fluctuations are massless as expected by Goldstone theorem. Along z direction, it is massive. Then, we get

$$\begin{aligned} ak^2\delta M_x(\mathbf{k}) - \beta H_x(\mathbf{k}) = 0, \\ ak^2\delta M_y(\mathbf{k}) - \beta H_y(\mathbf{k}) = 0, \\ (ak^2 - 2r)\delta M_z(\mathbf{k}) - \beta H_z(\mathbf{k}) = 0. \end{aligned}$$

This gives $\delta M_x(\mathbf{x}), \delta M_y(\mathbf{x}) \sim |\mathbf{x}|^{-1}$ and $\delta M_z(\mathbf{x}) \sim |\mathbf{x}|^{-1} e^{-\frac{|\mathbf{x}|}{\xi_f}}$. Here, we have demonstrated that the correlation function of a massless mode leads to long-range behaviors of the perturbations. Similar behavior exists in the perturbations to aligned conical phase in Sec. V B 2.

Here, we illustrate an example of a pure paramagnet with $q = 0$ and $H = 0$ here. In this case, $\mathbf{M}_0 = 0$. The kernel matrices are[29]

$$K_{ij}(\mathbf{k}) = \delta_{ij}(ak^2 - r).$$

Then

$$(ak^2 - r)\delta M_i(\mathbf{k}) - \beta H_i(\mathbf{k}) = 0,$$

for $i = x, y$ and z. This gives $\delta\mathbf{M}(\mathbf{x}) \sim |\mathbf{x}|^{-1} e^{-\frac{|\mathbf{x}|}{\xi_p}}$. Here we have demonstrated that if the correlation functions of all modes are massive, then the perturbations are short-ranged.

* kwyho@umd.edu

[1] T. H. R. Skyrme, Proc. Roy. Soc. London A **260**, 127 (1961)
[2] H. A. Fertig, L. Brey, R. Côté, A. H. MacDonald, A. Karlhede, and S. L. Sondhi, Phys. Rev. B **55**, 10671 (1997)
[3] C. Timm, S. M. Girvin, and H. A. Fertig, Phys. Rev. B **58**, 10634 (1998), cond-mat/9804057
[4] Q. Li, J. Toner, and D. Belitz, Phys. Rev. B **79**, 014517 (2009), arXiv:0711.4154
[5] T.-L. Ho, Phys. Rev. Lett. **81**, 742 (1998)
[6] L. S. Leslie, A. Hansen, K. C. Wright, B. M. Deutsch, and N. P. Bigelow, Phys. Rev. Lett. **103**, 250401 (2009)
[7] C. Thessieu, C. Pfleiferer, A. N. Stepanov, and J. Flouquet, J. Phys.: Condens. Matter **9**, 6677 (1997)
[8] A. Mühlbauer, B. Binz, F. Jonietz, C. Pfleiderer, A. Rosch, A. Neubauer, R. Georgii, and P. Böni, Science **323**, 915 (2009), arXiv:0902.1968
[9] C. Pfleiderer, A. Neubauer, S. Mühlbauer, F. Jonietz, M. Janoschek, S. Legl, R. Ritz, W. Münzer, C. Franz, P. G. Niklowitz, T. Keller, R. Georgii, P. Böni, B. Binz, and A. Rosch, J. Phys.: Condens. Matter **21**, 279801 (2009)
[10] X. Z. Yu, Y. Onose, N. Kanazawa, J. H. Park, J. H. Han, Y. Matsui, N. Nagaosa, and Y. Tokura, Nature **465**, 901 (2010)
[11] P. Bak and M. H. Jensen, J. Phys. C: Solid State Phys. **13**, L881 (1980)
[12] M. L. Plumer and M. B. Walker, J. Phys. C: Solid State Phys. **14**, 4689 (1981)
[13] I. E. Dzyaloshinski, J. Phys. Chem. Solids **4**, 241 (1958)
[14] T. Moriya, Phys. Rev. **120**, 91 (1960)
[15] K.-Y. Ho, T. R. Kirkpatrick, Y. Sang, and D. Belitz, Phys. Rev. B **82**, 134427 (2010), arXiv:1008.0134
[16] A. A. Belavin and A. M. Polyakov, Sov. Phys. JETP **22**, 245 (1975)
[17] A. Abanov and V. L. Pokrovsky, Phys. Rev. B **58**, R8889 (1998)
[18] M. Ezawa, Phys. Rev. Lett. **105**, 197202 (2010)
[19] A. N. Bogdanov and D. A. Yablonskiĭ, Sov. Phys. JETP **68**, 101 (1989)
[20] A. Bogdanov and A. Hubert, J. Mag. Mag. Mater. **138**, 255 (1994)
[21] A. Bogdanov, JETP Letters **62**, 231 (1995)
[22] U. K. Röβler, A. N. Bogdanov, and C. Pfleiderer, Nature **442**, 797 (2006)
[23] A. B. Butenko, A. A. Leonov, U. K. Röβler, and A. N. Bogdanov, Phys. Rev. B **82**, 052403 (2010), arXiv:0904.4842
[24] U. K. Röβler, A. A. Leonov, and A. N. Bogdanov, J. Phys.: Conf. Ser. **303**, 012105 (2011), arXiv: 1009.4849
[25] K. Everschor, M. Garst, R. A. Duine, and A. Rosch, Phys. Rev. B **84**, 064401 (2011)
[26] A. A. Abrikosov, Sov. Phys. JETP **5**, 1174 (1957)
[27] J. H. Han, J. Zang, Z. Yang, J.-H. Park, and N. Nagaosa, Phys. Rev. B **82**, 094429 (2010), arXiv:1006.3973
[28] T. R. Kirkpatrick and D. Belitz, Phys. Rev. Lett. **104**, 256404 (2010), arXiv:1003.4809
[29] S. K. Ma, *Modern Theory of Critical Phenomena* (Benjamin/Cummings, Reading, MA, 1976)
[30] D. Belitz and T. R. Kirkpatrick, Phys. Rev. B **81**, 184419 (2010)
[31] T. C. Lubensky, Phys. Rev. A **6**, 452 (1972)
[32] R. P. Feynman, A. R. Hibbs, and D. F. Styer, *Quantum Mechanics and Path Integrals* (Dover, Mineola, NY, NY, 2010)
[33] R. Rajaraman, *Solitons and Instantons* (Elsevier, New York, NY, 1987)
[34] P. G. de Gennes and J. Prost, *The Physics of Liquid Crystals* (Oxford University Press, New York, NY, 1993)
[35] C. Pfleiderer and A. Rosch, Nature **465**, 880 (2010)
[36] D. Forster, *Hydrodynamic Fluctuations, Broken Symmetry, and Correlation Functions*, Advanced Book Classics (Perseus, 1989)
[37] D. Belitz, T. R. Kirkpatrick, and A. Rosch, Phys. Rev. B **73**, 054431 (2006), cond-mat/0510444
[38] We do not consider the case for $H = 0$ because, while it does have a partial differential equation for δm_G, it is thermodynamically unstable as $\int d^3\mathbf{x} e^{i\mathbf{k}\cdot\mathbf{x}} \left(k_z^2 + \frac{\mathbf{k}_\perp^4}{2q^2}\right)^{-1} =$

$\sqrt{2}\pi q \int d^2\mathbf{k}_\perp \frac{1}{\mathbf{k}_\perp^2} e^{i\mathbf{k}_\perp\cdot\mathbf{x}_\perp} e^{-\frac{\mathbf{k}_\perp^2}{\sqrt{2}q}z}$, which is essentially equivalent to the Goldstone modes in $d = 2$, which leads to logarithmic divergence, according to Mermin-Wagner theorem.[43–45].

[39] J. F. Annett, *Superconductivity, Superfluids, and Condensates*, Oxford Master Series in Condensed Matter Physics (Oxford University Press, 2004)

[40] E. Fradkin, *Field Theories of Condensed Matter Systems* (Westview Press, 1998)

[41] A. M. Tsvelik, *Quantum Field Theory in Condensed Matter Physics* (Cambridge University Press, New York, NY, 2003)

[42] H. Kleinert, *Path Integrals in Quantum Mechanics, Statistics and Polymer Physics* (World Scientific, London, England, 1995)

[43] S. Coleman, Comm. Math. Phys. **31**, 259 (1973)

[44] P. C. Hohenberg, Phys. Rev. **158**, 383 (1967)

[45] N. D. Mermin and H. Wagner, Phys. Rev. Lett. **17**, 1133 (1966)